Expanding the clinical spectrum of *DRP2*-associated Charcot-Marie-Tooth disease

Sivera R[1,2], Pelayo-Negro AL[3,4], Jerico I[5], Dominguez C[2,6], Horga A[7], Rodriguez de Ribera FJ[8], Gallardo E[4,9], Tembl JI[1], Bermejo-Guerrero L[2,6], Pagola-Lorz I[5], Azorín I[10], Cordoba M[11], Fenollar M[12], Millet E[13], Vílchez JJ[10], Espinós C[2,14], Apellániz M[15], Sevilla T[1,2,16].

1) Servicio de Neurología, Unidad de Enfermedades Neuromusculares, Hospital Universitari i Politécnic La Fe. Grupo de Investigación en enfermedades neuromusculares y ataxias, Instituto de Investigación Sanitaria La Fe, Valencia. Spain

2) CIBER de enfermedades raras (CIBERER). Instituto de Salud Carlos III, Madrid. Spain.

3) Servicio de Neurología. Hospital Universitario Marqués de Valdecilla, Santander. Spain.

4) Centro de Investigación Biomédica en Red de Enfermedades Neurodegenerativas (CIBERNED). Instituto de Salud Carlos III, Madrid. Spain.

5) Departamento de Neurología, Hospital Universitario de Navarra, Instituto de Investigación Sanitaria de Navarra-IdiSNA, Pamplona. Spain.

6) Servicio de Neurología, Unidad de Enfermedades Neuromusculares, Hospital Universitario 12 de Octubre. Grupo de Investigación en Enfermedades mitocondriales y neuromusculares, Instituto de Investigación imas12, Madrid. Spain.

7) Servicio de Neurología. Hospital Clínico San Carlos. Instituto de Investigación Sanitaria del Hospital Clínico San Carlos de Madrid-IdISSC, Madrid. Spain.

8) Servicio de Neurología, Instituto de Investigación Sanitaria del Hospital Universitario La Paz – IDIPAZ, Hospital Universitario La Paz, Universidad Autónoma de Madrid, Madrid. Spain.

9) Servicio de Radiodiagnóstico. Hospital Universitario Marqués de Valdecilla, Santander. Spain.

10) Grupo de Investigación en enfermedades neuromusculares y ataxias, Instituto de Investigación Sanitaria La Fe, Valencia. Spain

11) Head of Neurology. Health in code.

12) Unidad de Genética Clínica, Servicio de Análisis Clínicos, Instituto de Medicina de Laboratorio, Hospital Clínico San Carlos. Instituto de Investigación Sanitaria del Hospital Clínico San Carlos de Madrid-IdISSC, Madrid. Spain.

13) Servicio de Neurofisiología, Unidad de Enfermedades Neuromusculares. Hospital Universitari i Politécnic La Fe. Grupo de Investigación en enfermedades neuromusculares y ataxias, Instituto de Investigación Sanitaria La Fe, Valencia. Spain.

14) Lab of Rare Neurodegenerative Diseases, Centro de Investigación Príncipe Felipe (CIPF), Valencia. Spain.

15) Unidad de Medicina Genómica, Instituto de Investigación Sanitaria de Navarra-IdiSNA, Universidad Pública de Navarra (UPNA), Pamplona. Spain.

16) Departamento de Medicina. Universitat de Valencia, Valencia. Spain

*Corresponding author:

Running title: *DRP2*-associated Charcot-Marie-Tooth disease

Number of figures: 4

Number of tables: 2

Supplemmenary material: 1 table

Number of references: 25

Summary

Background and Objectives: Germline truncating mutations in *DRP2* gene (encoding dystrophin-related protein 2) cause the disruption of the periaxin–DRP2–dystroglycan complex and have been linked to Charcot-Marie-Tooth (CMT) disease. However, the causality and the underlying phenotype of the genetic alterations are not clearly defined.

Methods: This cross-sectional retrospective observational study includes nine CMT patients with *DRP2* variants evaluated at six centers throughout Spain.

Results: We identified seven Spanish families with four different *DRP2* germline variants. In agreement with an X-linked inheritance, affected males presented with an intermediate form of CMT, while heterozygous women were asymptomatic. Symptom onset was variable (36,6 +/- 16 years), with lower limb weakness and multimodal sensory loss producing a mild to moderate functional impairment. Nerve echography revealed an increase in the cross-sectional area of nerve roots and proximal nerves. Lower limb muscle magnetic resonance imaging confirmed the presence of a length-

dependent fatty infiltration. Immunostaining in intradermal nerve fibers demonstrated the absence of DRP2 and electronic microscopy revealed abnormal myelin thickness that was also detectable in the sural nerve sections.

Discussion: Our findings support the causality of *DRP2* germline variants in CMT and further define the phenotype as a late-onset sensory and motor length-dependent neuropathy, with intermediate velocities and thickening of proximal nerve segments.

Keywords: Charcot-Marie-Tooth disease, *DRP2* gene, intermediate CMT.

Introduction

Charcot-Marie-Tooth disease (CMT) encompasses a group of genetically diverse inherited motor and sensory neuropathies. Typically, CMT is divided into demyelinating (CMT1 and CMT4) and an axonal forms (CMT2) according to motor nerve conduction velocity of the upper limbs[1]. The term intermediate CMT (I-CMT) was introduced to describe patients with clinical, electrophysiological and pathological features not fitting into either CMT1 or CMT2[2]. The electrophysiological limits of I-CMT have been controversial, Saporta *et al.*[3] restricted them to patients with upper limb motor nerve conduction velocity (NCV) of 35-45 m/s, and relatively preserved compound motor axon potential (CMAP). Genetic defects in *GJB1* gene are the most frequent cause of the X-linked form of I-CMT (OMIM # 302800), although pathogenic variants in other genes have also been described in I-CMT[4].

In 2015, a nonsense variant in *DRP2* (NM_001171184.2:c.805C>T p.Gln269*), the gene encoding dystrophin-related protein 2, was reported in a patient with late onset length-dependent sensorimotor neuropathy, electrophysiological characteristics of I-CMT, and absence of DRP2 protein in dermal nerves[5]. The same *DRP2* variant was subsequently detected in a patient with early adult-onset predominantly sensory neuropathy and myelin abnormalities in sural nerve biopsy, while the c.2214_c.2216del (p.Phe739del, NM_001939.3) variant was described in two Iranian siblings with childhood-onset axonal neuropathy and cardiomyopathy[6,7]. Furthermore, large deletions including *DRP2* have been described in individuals with X-linked agammaglobulinaemia and Mohr–Tranebjaerg syndrome, and the same variant (NM_001939.3:c.1294G>T p.Glu432*) has been detected in two cases with autism spectrum disorder[8,9,10].

DRP2 interacts with periaxin and dystroglycan to form the periaxin-DRP2-dystroglycan (PDG) complex. This complex is necessary for the formation of Cajal bands, which are cytoplasmic channels in the adhesion zones between the abaxonal surface of compact myelin and the Schwann cell plasma membrane[11]. Murine models confirm that loss of Drp2 disrupts the appositions and Cajal bands of myelinated nerves. These effects seem to be more pronounced with age, but are less prominent than in the periaxin knockout models, and do not alter internodal lengths, conduction velocities or motor behavior[12].

In this study, we identified Spanish patients with I-CMT and *DRP2* genetic variants supporting the involvement of this gene in CMT and expanding the known phenotype.

Methods

This cross-sectional multicenter retrospective observational study enrolled all patients with *DRP2* germline variants associated with CMT disease across six medical centers throughout Spain. The patients were identified through collaboration within the Neuromuscular Work Group of the Spanish Neurology Society (SEN), and a national register of hereditary neuropathies. All patients and relatives included in the present study signed informed consent, and the research protocols were approved by the institutional ethics committees of the corresponding hospitals. Photographs and videos of the patients were taken and reproduced only after specific informed consent.

A standardized history and symptom questionnaire was employed to collect the basal information. The severity of the neuropathy was evaluated using the CMT neuropathy score version 1 (CMTNS) as a significant proportion of the patients had not undergone the mandatory neurophysiologic radial nerve testing required for version 2[13]. For

patients without nerve conduction studies, the CMT examination score (CMTES) was employed. Motor and sensory nerve conduction studies (NCS) were performed using standard techniques with controlled temperature at or above 32ºC.

Genetic studies were performed at the genetic departments of the hospitals involved, Centro de Investigación Principe Felipe (Valencia, Spain), Navarrabiomed (Pamplona, Spain) and Health In Code Group (Valencia, Spain). Germline DNA was extracted from peripheral blood samples from the individuals using commercially available kits. *DRP2* variants were identified using gene panels including CMT associated genes, whole exome sequencing (WES) or whole genome sequencing (WGS), filtering variants according to existing protocols[14].

To test the impact of splicing variants, when possible, total RNA was extracted from patients' lymphocytes using Trizol Reagent (Thermo Fisher Scientific). RNA was reverse transcribed into cDNA with SuperScript III First-Strand Synthesis System and random hexamers (Thermo Fischer Scientific). PCR was performed on cDNA to amplify the region spanning exon 5 to exon 7 of *DRP2*. PCR reactions were separated on 2% agarose gels and each band was obtained using QIAquick Gel Extraction Kit (Qiagen), followed by Sanger sequencing.

Segregation analysis was performed in the available family members. All *DRP2* variants have been classified following the American College of Medical Genetics (ACMG) guidelines[15]. *In silico* splicing prediction programs SpliceAI, Human Splicing Finder and dbscSNV algorithms were used. Resources such as ClinVar (https://www.ncbi.nlm.nih.gov/clinvar/), VarSome (https://varsome.com/), and Franklin (https://franklin.genoox.com/clinical-db/home) were employed. Also, the Genome Aggregation Database (gnomAD) was consulted to determine the relative frequency of

the identified *DRP2* variants in the general population[16].

Muscle magnetic resonance imaging (MRI) of the feet and lower limbs was performed in five patients, and the protocol was described previously[17]. Muscle fatty substitution was graded from 0 to 4 according to the modified Mercuri score[18]. MRI of the lumbar spine with reconstruction of the lumbosacral plexus was performed in one patient.

Ultrasound examinations of the peripheral nerves of four patients were completed in two of our sites using the same protocol[19]. The studies were performed using a Toshiba Aplio XG (Tokyo, Japan 2008) and a Canon Medical Systems Aplio i700 (Otawara, Japan 2020) echograph; equipped with a high-frequency broadband probe up to 18 MHz. In each nerve, the cross-sectional area (CSA) was determined in axial planes by tracing nerves just inside their hyperechoic rims. We obtained bilateral measurements of the nerve roots C5-C7, the median, ulnar and radial nerves in the arm and forearm as well as the sural, peroneal and posterior tibial nerves in the lower limbs, and compared them with control values. Cut-off values for abnormal CSA were derived from normative data of our laboratory and defined as the upper limit [20,21]. We also recorded the morphology and echogenicity of the fascicular pattern in the different nerve sites. Analysis of data from ultrasonography was performed both online and offline, using the Image J software (NIH, Bethesda, MD, USA).

Skin biopsies were obtained using a 3 mm punch from glabrous skin of the lateral aspect of the thigh. For immunofluorescence assays, samples were fixed in 4% paraformaldehyde in PBS overnight at 4ºC, gradually immersed in sucrose for cryoprotection and frozen in liquid nitrogen. Sections were washed by stirring in PBS (1% BSA 4% NGS 0.4% Triton) for 2 hours at room temperature and incubated with primary antibody overnight in the same buffer (anti-DRP2 was kindly gifted by Dr.

Peter Brophy and Dr. Diane Sherman; Anti-Myelin Basic Protein (PBM) Millipore-Sigma MAB 382, Burlington, MA, USA). They were then incubated by stirring with the secondary antibody for 2 hours at room temperature (Alexa Fluor 488 chicken anti-mouse IgG (H+L) Invitrogen A21200 and Alexa Fluor 555 goat anti-rabbit IgG (H+L) Invitrogen A21428, Waltham, MA, USA). Sections were frozen and prepared for a laser confocal SP5 microscope, and images were obtained using a 40x objective. Skin samples destined for EM were fixed in 0.8% paraformaldehyde and 2% glutaraldehyde in PBS 5 h at 4ºC and then osmicated in 1% osmium tetroxide for 2 hours, dehydrated, and embedded in epoxy resin (epon). Tissue blocks were then trimmed and stained with lead citrate and uranyl acetate. Images were obtained with Transmission electron microscope FEI Tecnai Spirit BT (ThermoFisher Scientific company, Waltham, MA, USA).

A sural nerve and *gastrocnemius* muscle biopsy was performed under local anesthesia in patient 7 according to standard protocols[22].

Results

Nine CMT patients, belonging to seven different families, with presumably causative variants in *DRP2* were identified and assessed, along with eight asymptomatic female carriers.

Genetic studies:

Four different *DRP2* germline variants were detected. Two alterations were nucleotide changes resulting in a missense and a nonsense variant, while the other two were intronic deletions predicted to result in the skipping of exon 6 (figure 1, table 1). The c.1294G>T

(p.Glu432*; rs759517614) change was detected in three families (five patients). The variant segregated with the disease and five carrier women were identified, none of which were symptomatic by clinical history, neurological examination or NCS. This nonsense variant was classified as pathogenic (ClinVar ID: 1360406 and ACMG criteria met: PVS1_Very strong, PM2_Moderate). In gnomAD, this variant presents a minor allele frequency (MAF) of 0.0104% with 9 hemizygous males out of 125,688 individuals, being slightly more frequent in Latino/Admixed population MAF =0.062% (gnomAD; accessed April 2023). Moreover, two different *DRP2* deletions were detected in three sporadic patients, c.559+3_559+16del and c.439-123_559+197del. Both were predicted with *in silico* tools to affect the canonical splicing, leading to a premature stop codon (p.Ala157Ilefs*29). Indeed, the analysis of patient's and relatives' RNA showed that both intronic variants resulted in skipping of exon 6. These variants segregated with the disease and were predicted to be likely pathogenic (ACMG for c.559+3_559+16del: PVS1, PM2; and ACMG CNV c.439-123_559+197del: 1A, 2B, 2E, 3A). They were not described in gnomAD nor in ClinVar. Finally, the c.1790G>A (p.Arg597Gln) variant was detected in a sporadic patient, and classified as variant of uncertain significance (VUS; ACMG: PP3, PM2), and not reported in gnomAD.

Clinical assessments:

The demographic and clinical characteristics are detailed in table 1 and figure 2. All affected males exhibited symptoms, except for one young patient (case 8), who considered himself asymptomatic but exhibited areflexia and mild atrophy of the intrinsic foot muscles in the clinical examination and unequivocal alterations in NCS. The mean age of symptom onset was 36.5 years (15-58 years) referring walking difficulties, frequent stumbling and distal lower limb weakness. Disease progression was relatively mild in most patients, but at least two patients (case 1 and 2) experienced

a moderately rapid decline with significant distal weakness and multimodal sensory loss causing substantial disability (supplementary video 1). Globally, weakness was length dependent, affecting the distal lower limbs in all symptomatic patients, while only two patients exhibited clear weakness of the intrinsic hand muscles and none had proximal involvement. Multimodal sensory loss was present in 7 out of 9 patients in the lower limbs, while sensory ataxia was reported in only three patients.

Nerve conduction studies:

Table 2 provides a detailed summary of the NCVs, which demonstrated a length-dependent sensory and motor polyneuropathy. Motor upper limb NCVs were within the axonal or intermediate ranges (median 31.2-47.2 m/sec, ulnar 35.5-47.2 m/sec), while CMAP amplitude was decreased prominently in lower limb nerves and concordantly with disease severity. Distal latencies were prolonged in 60% of the tested nerves, and F waves were either prolonged or absent in all ten tested nerves. Sensory nerve conduction studies revealed a reduction in SNAP (Sensory Nerve Action Potential) amplitudes in practically all tested nerves, with a mild to moderate reduction of conduction velocities.

Nerve ultrasound and magnetic resonance imaging:

Nerve ultrasound was performed in patients 1, 2, 3 and 8. Cross sectional area was globally increased in all the nerves tested compared to control values, as is shown in figure 3 and supplementary table 1. The cervical root CSA was markedly increased in all tested patients: C5 13.9 (7-16) mm^2, C6 20.8 (18-27) mm^2, C7 18.1 (14-22) mm^2 compared with control values (8.3, 11.9 and 12.8 mm^2 respectively) as was the median, radial and ulnar nerves above the elbow. In the distal nerve segments of the upper limb the increase in CSA was milder like the median nerve in the forearm (8.9 [7-12] mm^2

*vs.*7.1 mm^2). In the lower limbs, the proximal CSA of the popliteal sciatic nerve was significantly increased (36 [30-41] mm^2 *vs.* 23.1 mm^2) as was the peroneal nerve in the popliteal fossa, while the thickening was less prominent in the distal segments (sural nerve 3.8 [2-6] mm^2 *vs.* 3 mm^2). The morphology of the fascicular pattern was abnormal in certain nerves, sometimes detecting the presence of one or two remarkably enlarged fascicles, or others where there was a mild increase in echogenicity of the fascicular pattern (figure 3).

Lumbar spine MRI with lumbosacral plexus reconstruction revealed a homogeneous thickening of all the lumbar nerve roots in patient 8, who was asymptomatic at that time. This test was performed due to a possible sacroiliitis associated with HLAB27, and in fact these findings were what initially motivated the referral to the neurology clinic. Lower limb muscle MRI was performed in patients 1, 2, 3, 8 and 9. Fatty muscle infiltration could be identified in all cases except in patient 8, who was asymptomatic and the only abnormalities were a subtle decrease of the muscle volume of the feet. In the other four patients there was clear length dependent fatty replacement, affecting the muscles of the feet and the distal segments of the calves, being concordant with disease severity. There was not a clear pattern of muscle infiltration in the calf, although the deep posterior compartment (*tibialis posterior, flexor digitorum longus,* and *flexor hallucis longus*) seemed to be more preserved than the anterior and lateral compartment until later stages of the disease (figure 3).

Pathology:

Skin biopsy was performed in patients 1, 2 and 3 (p.Glu432*) and compared with controls. In the subjects there was a consistent lack of DRP2 staining in all myelinated fibers (figure 4) compared to controls in which DRP2 immunofluorescence colocalized

with myelin basic protein (MBP). Nerve fiber architecture was evaluated using electron microscopy and we detected decompaction of myelin, as well as a circumferential band of Schwann cell cytoplasm surrounding the abaxonal myelin in most myelinated axons. In some of the fibers axonal vacuoles and inclusion bodies were identified near the Cajal bands of myelinated axons. Sural nerve and *gastrocnemius* muscle biopsy were performed in patient 7, when he was 38 years old. The sural nerve showed an important loss of large myelinated fibers, demyelinated axons and occasional segmentally thickened myelin sheath (tomaculous change). The muscle biopsy revealed a neurogenic pattern of muscle fiber atrophy, unfortunately we do not have available images.

Discussion

Loss of function *DRP2* mutations have been proposed as a potential cause of intermediate X-linked CMT causing the disruption of the PDG complex[5]. Since the first publication in 2015, only two additional cases of *DRP2*-related neuropathies have been reported, and the underlying phenotype is not clearly established[6,7]. Here we present a clinically well-defined series of seven Spanish pedigrees with intermediate CMT phenotype and germline *DRP2* variants, three of them novel

All affected males in our cohort were symptomatic except for the youngest patient (21 years and hemizygous for c.439-123_559+197del), while heterozygous women were healthy. Age of onset was variable, but in 60% of the cases, neuropathy symptoms appeared after the 4th decade, usually with lower limb distal weakness. Progression was mostly mild, but in two cases there was a quick worsening hampering independent ambulation. Muscle weakness was symmetrical and length dependent, affecting

exclusively the distal leg muscles in most patients, while only two had intrinsic hand muscle involvement, and none had proximal weakness. Sensory impairment could be detected in more than 75% of the patients but sensory ataxia was not the most prominent feature, as had been previously described[6]. We also did not detect any features of autism spectrum disorder or cardiomyopathy, as had been previously reported[7,9]. NCVs were consistent throughout the whole series independently of the genotype, age, or severity. The electrophysiologic signature consisted of mildly reduced motor NCVs in the upper limb nerves (axonal or intermediate range), while distal latencies and F-waves were usually prolonged. All the studied women carriers of *DRP2* variants in heterozygosity had normal NCVs.

Echography is an increasingly used technique that allows for excellent visualization of the peripheral nerve, including proximal sections that are difficult to assess with standard nerve conduction studies[23]. The utility in CMT is being recognized specially in the distinction between different subtypes and to discard alternative diagnosis. We performed nerve echography to four patients with different ages and genotypes, finding a marked increase in CSA of cervical nerve roots and proximal nerves of the upper limbs, while the distal segments and lower limb nerves were only mildly thickened. This pattern differs from that of CMT1A and other demyelinating subtypes, where CSA is homogeneously increased in all nerves, and also from most CMT2 subtypes, where it is normal or mildly reduced. However, it may be similar to that of CMTX, with a moderate symmetrical increase of CSA in proximal upper limb nerve segments and variable involvement of distal segments and lower limb nerves[24,25].

In any case, it is a clinically relevant appreciation that *DRP2* germline pathogenic variants may lead to a late onset neuropathy where the identification of proximal nerve thickening may raise the suspicion of an alternative diagnosis like inflammatory or

neoplastic neuropathy. In fact, the patient reported by Brennan *et al.* (2015) was initially diagnosed with an acquired demyelinating neuropathy, and thus treated with immunomodulatory treatments[5]. A clear paradigm of this is patient 8, where the proximal thickening of the lumbar plexus nerve roots detected in a lumbar MRI was what prompted the neurological evaluation before neuropathy became symptomatic.

The physiopathology underlying *DRP2*-related neuropathy is not clearly understood. Murine models suggest that the disruption of the PDG complex in appositions that define the boundaries of the Cajal bands alters the regulation of the radial growth of myelin. Drp2 mutants had normal internodal lengths, conduction velocities, and motor behavior, but abnormal profiles in the mutant appeared with increasing age, finding a higher proportion of nerves with focal hypermyelination and demyelination[12]. Similar findings were identified in a sural nerve biopsy of a patient with the p.Gln269* variant in *DRP2*, with prominent variability in myelin thickness including many thinly myelinated fibers and other abnormally thickened, very similar to that of our patient with the c.559+3_559+16del exon 6 deletion [6]. Skin biopsies performed in three patients with the p.Glu432* variant enabled us to confirm the lack of DRP2 staining in all myelinated nerves, and also to confirm the structural abnormalities of the myelinated fibers.

The most common variant detected in our series is *DRP2* c.1294G>T (p.Glu432*), present in four patients from three families that live in different Spanish regions. This nucleotide change was classified as deleterious in the different databases, and has been reported as pathogenic in ClinVar (ID: 1360406) but was also present in nine presumably healthy males in gnomAD. This is probably due to the late onset of the disease and the symptomatic mildness. We cannot completely exclude an incomplete penetrance but in our series all male carriers were clearly affected. We also detected two

different novel deletions encompassing intronic sequences that affect splicing canonical sites leading to a frame-shift and a premature stop codon (p.Ala157Ilefs*29), with indistinguishable phenotypic characteristics from the other variants. Finally, the c.1790G>A (p.Arg597Gln) is a missense VUS present in his asymptomatic mother, we lack functional studies that back the pathogenicity of this variant but the concordant clinical presentation and the electrophysiological and muscle MRI findings support it.

This report provides further evidence on the causality of *DRP2* germline pathogenic variants in I-CMT and expands the known phenotype. The characteristic clinical picture in our series was an adult onset length-dependent sensory and motor neuropathy with intermediate velocities, prolonged latencies and thickening of proximal nerve segments.

Acknowledgements

We deeply appreciate the commitment of the families studied. Cristina Domínguez-González, Teresa Sevilla, and Rafael Sivera are members of the European Reference Network for rare neuromuscular diseases (ERN-MND).

Funding

This collaborative joint project

MA-R is supported by a Postdoctoral Junior Leader - INCOMING fellowship from La Caixa Foundation (ID 100010434) and from the European Union's Horizon 2020 research and innovation programme under the Marie Skłodowska Curie grant agreement

No. 847648. MA-R fellowship code is LCF/BQ/PI21/11830009. This work was supported by the Carlos III Health Institute (ISCIII), [Grant PI21/00103 to CE], and co-funded by the European Union—European Regional Development Fund (ERDF) and the European Social Fund (FSE) 'A way of making Europe'.

References

1) Harding A, Thomas PK. The clinical features of hereditary motor and sensory neuropathy types I and II. *Brain*. 1980;103:259-280; doi:10.1093/brain/103.2.259.
2) Davis CJ, Bradley WG, Madrid R. The peroneal muscular atrophy syndrome: clinical, genetic, electrophysiological and nerve biopsy studies. I. Clinical, genetic and electrophysiological findings and classification. *J Genet Hum*. 1978;26:311-349; PMID: 752065.
3) Saporta AS, Sottile SL, Miller LJ, Feely SM, Siskind CE, Shy ME. Charcot-Marie-Tooth disease subtypes and genetic testing strategies. *Ann Neurol*. 2011;69: 22-33; doi:10.1002/ana.22166.
4) Berciano J, García A. Gallardo E, *et al*. Intermediate Charcot-Marie-Tooth disease: an electrophysiological reappraisal and systematic review. *J Neurol*. 2017;264:1655-1677; doi:10.1007/s00415-017-8474-3.
5) Brennan KM, Bai Y, Pisciotta C, *et al*. Absence of Dystrophin Related Protein-2 disrupts Cajal bands in a patient with Charcot-Marie-Tooth disease. *Neuromuscul Disord*. 2015;25:786-793; doi:10.1016/j.nmd.2015.07.001.
6) Roda RH, McCray BA, Klein CJ, Hoke A. Novel hemizygous nonsense mutation in DRP2 is associated with inherited neuropathy. *Neurol Genet*. 2018;4:e220; doi:10.1212/NXG.0000000000000220.
7) Tahmasebi-Birgani M, Hajjari M, Golchin N, Shalbafan B, Mohammadi-Asl J, Sadeghian F. Whole exome sequencing revealed a novel dystrophin-related protein-2 (*DRP2*) deletion in an Iranian family with symptoms of polyneuropathy.

Iran J Basic Med Sci. 2019;22:576-580; doi:10.22038/ijbms.2019.30754.7414.

8) Sediva A, Smith CI, Asplund AC, *et al*. Contiguous X-chromosome deletion syndrome encompassing the BTK, TIMM8A, TAF7L, and DRP2 genes. *J Clin Immunol*. 2007;27:640-646; doi:10.1007/s10875-007-9123-x.
9) Lim ET, Raychaudhuri S, Sanders SJ, *et al*. Rare complete knockouts in humans: population distribution and significant role in autism spectrum disorders. *Neuron*. 2013;77:235-242; doi:10.1016/j.neuron.2012.12.029.
10) Toma C, Torrico B, Hervas A, *et al*. Exome sequencing in multiplex autism families suggests a major role for heterozygous truncating mutations. *Mol Psychiatry*. 2014;19:784-90; doi:10.1038/mp.2013.106.
11) Shermann DL, Wu LM, Grove M, Gillespie CS, Brophy PJ. Drp2 and periaxin form Cajal bands with dystroglycan but have distinct roles in Schwann cell growth. *J Neurosci*. 2012;32:9419-28; doi:10.1523/JNEUROSCI.1220-12.2012.
12) Sherman DL, Brophy PJ. A murine model of Charcot-Marie-Tooth disease 4F reveals a role for the C-terminus of periaxin in the formation and stabilization of Cajal bands. *Wellcome Open Res*. 2018;3:20; doi:10.12688/wellcomeopenres.13673.1.
13) Murphy SM, Herrmann DN, M Dermott MP, et al. Reliability of the CMT neuropathy score (second version) in Charcot-Marie-Tooth disease. *J Peripher Nerv Syst*. 2011;16:191-198; doi:10.1111/j.1529-8027.2011.00350.x.
14) Sánchez-Monteagudo A, Álvarez-Sauco M, Sastre I, *et al*. Genetics of Wilson disease and Wilson-like phenotype in a clinical series from eastern Spain. *Clin Genet*. 2020;97:758-763; doi:10.1111/cge.13719.
15) Richards S, Aziz N, Bale S, *et al*. Standards and guidelines for the interpretation of sequence variants: a joint consensus recommendation of the American College of Medical Genetics and Genomics and the Association for Molecular Pathology. *Genet Med*. 2015;17:405-24; doi:10.1038/gim.2015.30.
16) Karczewski KJ, Francioli LC, Tiao G, *et al*. The mutational constraint spectrum quantified from variation in 141,456 humans. *Nature*. 2020;581:434-443; doi:10.1038/s41586-020-2308-7.
17) Muelas N, Frasquet M, Más-Estelles F, *et al*. A study of the phenotypic variability and disease progression in Laing myopathy through the evaluation of muscle imaging. *Eur J Neurol*. 2021;28:1356-1365; doi:10.1111/ene.14630.
18) Fischer D, Kley RA, Strach K, *et al*. Distinct muscle imaging patterns in

myofibrillar myopathies. *Neurology* 2008;71:758-765. doi:10.1212/01.wnl.0000324927.28817.9b.

19) Gallardo E, Sedano MJ, Orizaola P, *et al*.. Spinal nerve involvement in early Guillain-Barré syndrome: a clinico-electrophysiological, ultrasonographic and pathological study. *Clin. Neurophysiol.* 2015;126:810–819; doi:10.1016/j.clinph.2014.06.051.
20) Drake-Pérez M, Pelayo-Negro AL, Sánchez-de la Torre JR, Berciano J, Gallardo E. Ultrasonography of cervical nerve roots: cross-sectional reference values according to age. *Neurol Sci*. 2021; 42:215-223; doi:10.1007/s10072-020-04551-x.
21) Drake M. Mapa neural ecográfico de la Comunidad de Cantabria: Valores de referencia (Doctoral dissertation). Universidad de Cantabria 2021.
22) Garcia-Bragado F, Fernandez JM, Navarro C, Villar M, Bonaventura I. Peripheral neuropathy in essential mixed cryoglobulinemia. Arch Neurol. 1988;45:1210-1214; doi:10.1001/archneur.1988.00520350048015.
23) Padua L, Coraci D, Lucchetta M, *et al*. Different nerve ultrasound patterns in charcot-marie-tooth types and hereditary neuropathy with liability to pressure palsies. *Muscle Nerve*. 2018;57:E18-E23; doi:10.1002/mus.25766.
24) Grimm A, Rasenack M, Athanasopoulou IM, Dammeier NM, Lipski C, Wolking S, et al. The modified ultrasound pattern sum score mUPSS as additional diagnostic tool for genetically distinct hereditary neuropathies. *J Neurol* 2016;263:221-230; doi:10.1007/s00415-015-7953-7.
25) Zanette G, Fabrizi GM, Taioli F, Lauriola MF, Badari A, Ferrarini M, Cavallaro T, Tamburin S. Nerve ultrasound findings differentiate Charcot-Marie-Tooth disease (CMT) 1A from other demyelinating CMTs. Clin Neurophysiol. 2018 Nov;129(11):2259-2267; doi:10.1016/j.clinph.2018.08.016.

Table 1: Demographic and clinical characteristics.

Table 2: Nerve conduction studies.

Supplementary videos: patient 1 and 2

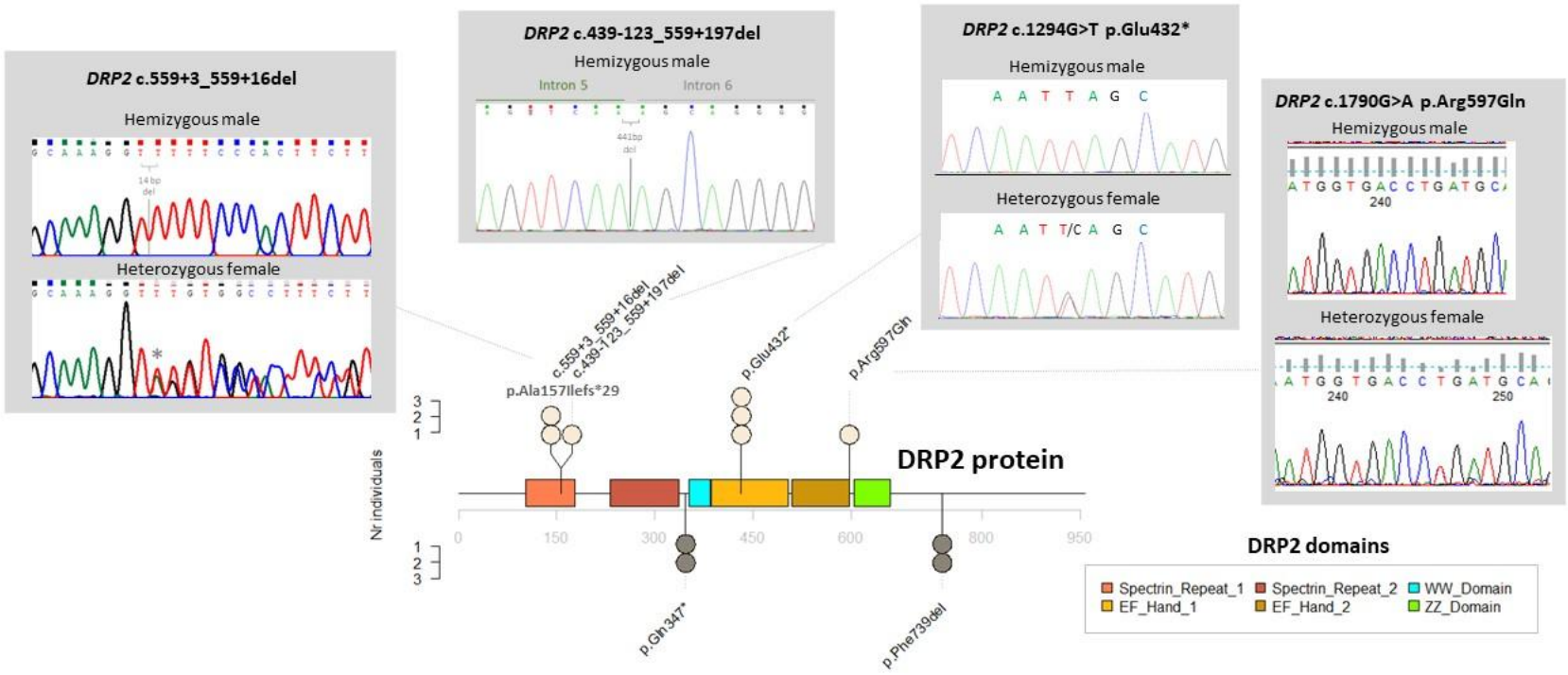

Nr patients	Onset	Phenotype	cDNA change	Protein change	Reference
1	18y	Numbness and tingling in toes. Sensory loss light touch, pinprick, temperature. Strength normal.	#NM_001171184:c.805C>T	NP_001164655: p.Gln269*	Roda *et al.*
1	50y	Typical sensorimotor CMT starting with foot drop, remarkable sensory loss mainly vibratory.	#NM_001939:c.1039C>T	NP_001930: p. Gln347*	Brennan *et al.*
2	Childhood	Sensorimotor polyneuropathy. Consanguinity.	NM_001939:c.2214_2216del	NP_001930: p.Phe739del	Tahmasebi-Birgani *et al.*

The *DRP2* variants identified in Roda *et al* and Brennan *et al* correspond to the same change in the DNA sequence but they use a different transcript for nomenclature.

Fig. 1. Chromatography of DRP2 variants detected and localization in protein.

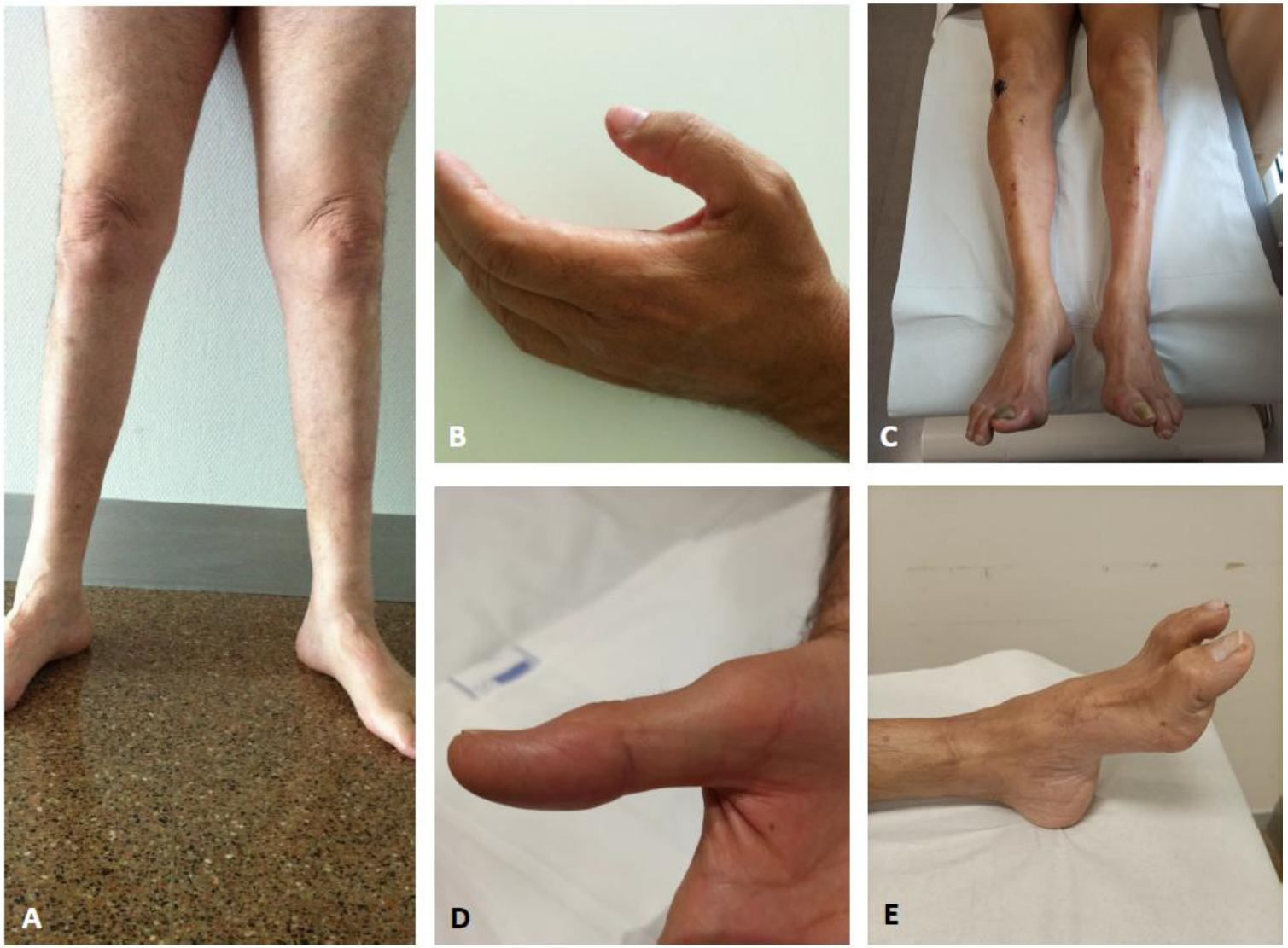

Fig. 2. Clinical features of the DRP2 associated neuropathy. A and B: Legs and hand photographs of patient 1 with marked distal atrophy of calves and feet as well as 1rst interosseus and thenar eminence, *pes cavus*. Cand D: Legs and hand photographs of patient with atrophy in the distal calves and feet, and very mild in the thenar eminence. E: Left foot of patient 3, with intrinsic foot muscle atrophy, *pes cavus* and hammer toes.

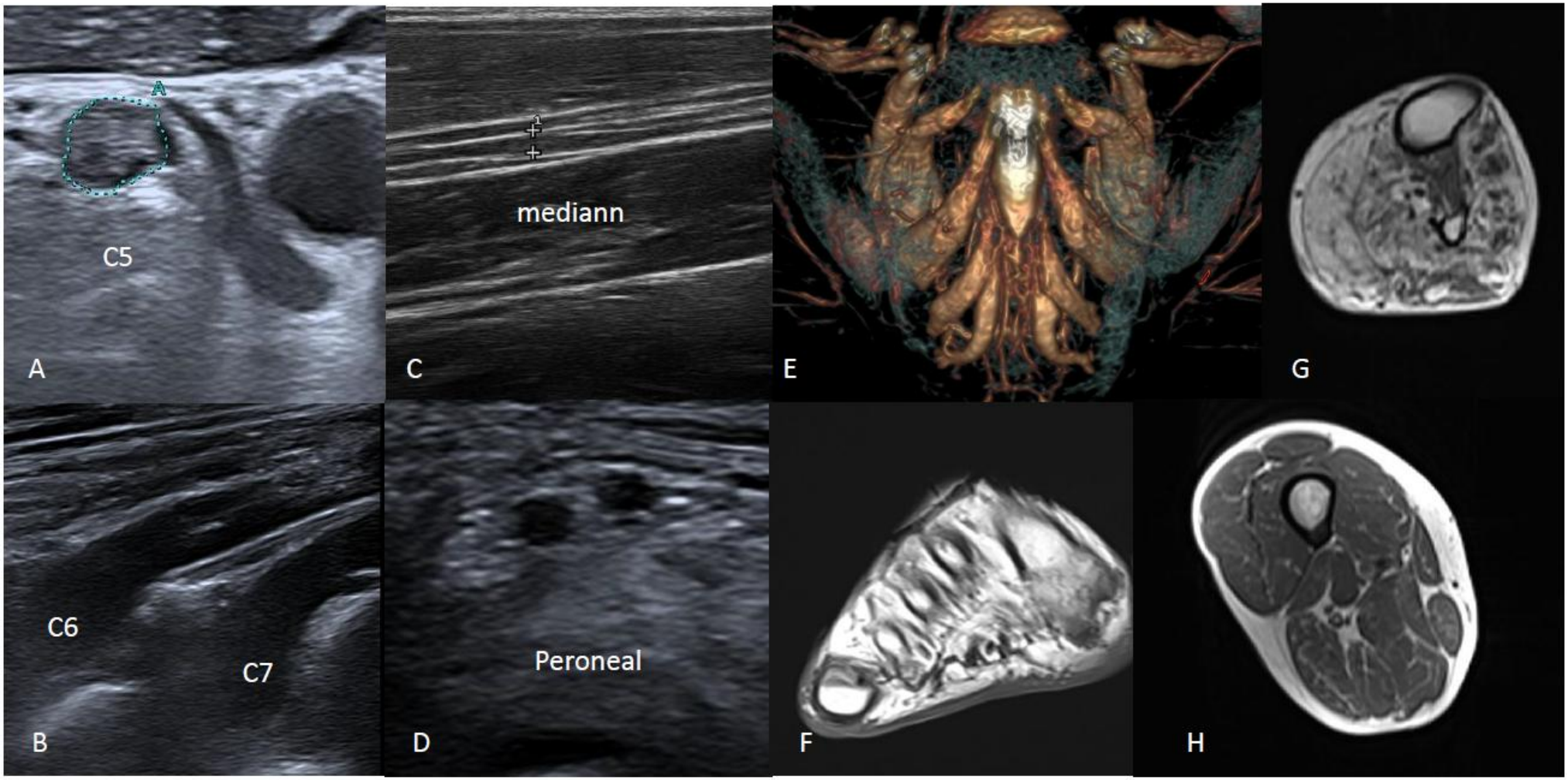

Fig 3. Nerve echography, MR with 3D reconstruction of the lumbosacral plexus and MR of lower limb muscles. A: Echography of C5 nerve root, transversal plane used for the measurement of CSA. B: Echography of C6 and C7 nerve roots of patient 1, longitudinal plane with proximal thickening. C: Median nerve of patient 2 with a mild increase in echogenicity of the fascicular pattern. D: Peroneal nerve of patient 3 with abnormal fascicular pattern, with two remarkably enlarged fascicles. E: 3D reconstruction of the lumbosacral plexus pf patient 8, with marked enlargement of all nerve trunks. F,G,H: Lower limb muscle MR of patient 3, with complete fatty substitution in the intrinsic foot muscles, important atrophy and fat replacement in calf muscles, with relative preservation of the deep posterior compartment and thigh muscles.

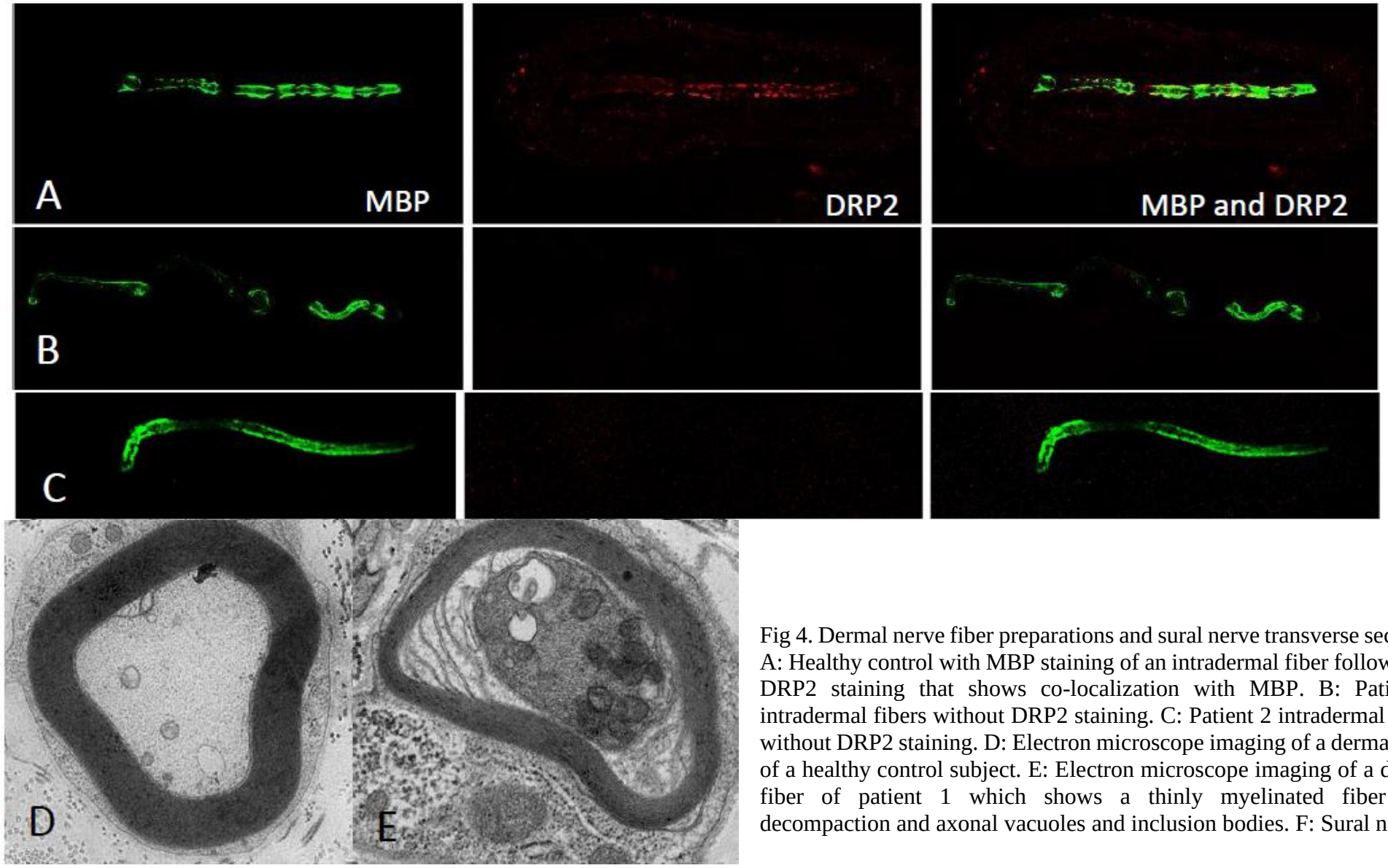

Fig 4. Dermal nerve fiber preparations and sural nerve transverse sections. A: Healthy control with MBP staining of an intradermal fiber followed by DRP2 staining that shows co-localization with MBP. B: Patient 1 intradermal fibers without DRP2 staining. C: Patient 2 intradermal fibers without DRP2 staining. D: Electron microscope imaging of a dermal fiber of a healthy control subject. E: Electron microscope imaging of a dermal fiber of patient 1 which shows a thinly myelinated fiber with decompaction and axonal vacuoles and inclusion bodies. F: Sural nerve.

Table 1 (valorar incluir columna de VUS/pahogenic…)

Case	Nomenclature HGVS - cDNA	Nomenclature HGVS - Protein	Onset (ys)	Age	Motor		Sensory		Reflexes	Sensory ataxia	Foot deformities	CMTNS CMTES	Functional situation (ys)
					UL	LL	UL	LL	UL/LL				
1	c.1294G>T	p.Glu432*	Stumbling, LL distal weakness (20)	62	5/3	5/0	T,V	T, Pa, Po,V	0/0	No	Pes cavus Hammer toes	25/21	Two crutches (50)
2	c.1294G>T	p.Glu432*	Stumbling, trouble walking (47)	64	5/5	5/2	N	T, Pa, V	+/0	Yes	Pes cavus Hammer toes	15/11	DAFO (60)
3	c.1294G>T	p.Glu432*	Right foot drop (35)* Bilateral LL distal weakness (50)	67	5/5	5/<2	N	T, Pa, V	0/0	Yes	Pes cavus Hammer toes	13/11	DAFO (55)
4	c.1294G>T	p.Glu432*	LL distal weakness, tingling (43)	63	5/5	5/4	N	V	+++/+++ **	No	Pes cavus	3/3	Walks unaided
5	c.1294G>T	p.Glu432*	Stumbling, trouble walking (58)	66	5/5	5/4	N	N	0/0	No	No	5/3	Walks unaided
6	c.559+3_559+16del	p.(Ala157Ilefs*29)	Stumbling, trouble walking (40)	76	5/3	5/0	T, Pa, V	T, Pa, V	0/0	No	Pes cavus	21/15	DAFO (52) One crutch (66)
7	c.559+3_559+16del	p.(Ala157Ilefs*29)	Stumbling, trouble walking (15)	66	5/4	5/3	T	T,V	+/0	No	Pes cavus Hammer toes	15/11	DAFO (53)
8	c.439-123_559+197del	p.(Ala157Ilefs*29)	Asymptomatic	21	5/5	5/5	N	N	0/0	No	No	1/0	N
9	c.1790G>A	p.Arg597Gln	Stumbling, trouble walking (19)	54	5/5	5/3	N	T, V	+/0	Yes	Pes planus	15/14	DAFO (50)

Patients 1 and 2 are siblings, as are 4 and 5. HGVS: Human Genome Variation Society, ys: years, UL: Upper limb proximal/distal MRC scores, LL: Lower limb proximal/distal MRC scores. CMTNS: CMT neuropathy score version 1, CMTES: CMT examination score, T: Tactile, Pa: Pain, Po: Positional, V: Vibratory, N: Normal, DAFO: Dynamic ankle foot orthosis. * Subacute foot drop attributed to a L5 herniated disc. ** Probably due to a previous cervical myelopathy. *DRP2* transcript used NM_001939.3.

Table 1

Case	Nomenclature HGVS - cDNA	Current age / onset	Motor median				Motor ulnar				Motor peroneal					Sensory ulnar		Sensory median		Sural	
			CMAP	CV	DL	F-wave	CMAP	CV	DL	F-wave	CMAP	CV	DL	F-wave		SNAP	CV	SNAP	CV	SNAP	CV
1	c.1294G>T	57/37	0.6	-	8,7	NP	7	39,1	4,3	40,2	A	-	-	-		A	-	A	-	A	-
2	c.1294G>T	64/17	7,4	47,2	3,3	37,6	6,7	47,2	3,4	38,5	0,9	-	4,1	NP		2,5	43,8	A	-	0,6	36,5
3	c.1294G>T	67/32	4,4	31,2	5,6	NP	8,1	35,5	3,9	40	A	-	-	-		3,1	36,7	2,3	36,8	3,9	33,3
4	c.1294G>T	54/11	NP	NP	NP	NP	7,7	40,7	2,95	43,8	1,8	33	5,8	NP		10,4	40	14,2	50	10,3	53,3
5	c.1294G>T	65/7	9,5	41,9	9,9	NP	10,4	40,8	8,3	NP	NP	NP	NP	NP		4,2	42,9	4,2	42,3	1,7	44,1
6	c.559+3_559+16del	43/3	3	34	4,9	NP	4	46	3,6	NP	A	-	-	-		NP	NP	A	-	A	-
7	c.559+3_559+16del	38/23	12	46	3,9	NP	14	46	3,3	NP	A	-	-	-		NP	49	7	49	NP	NP
8	c.439-123_559+197del	21/A	7,4	40,7	3,9	38,5	9	42,6	2,6	39,6	9	25,3	7,2	85,6		7,8	39,7	11,3	39,2	10,7	37,3
9	c.1709G>A	47/28	6,5	43	4,3	34,5	7,7	44,7	3	38,2	A	-	-	-		4,1	44,4	6,7	49,2	A	-

HGVS: Human Genome Variation Society, CMAP: in mV, CV: in m/s, DL: in sec, F-wave: in sec, SNAP: in mV, NP: Not performed, A: Absent. DRP2 transcript used NM_001939.3.